ESAIM: M2AN
Vol. 39, N° 2, 2005, pp. 319–348
DOI: 10.1051/m2an:2005009

ESAIM: Mathematical Modelling and Numerical Analysis

A POSTERIORI ERROR ESTIMATES FOR A NONCONFORMING FINITE ELEMENT DISCRETIZATION OF THE HEAT EQUATION

Serge Nicaise[1] and Nadir Soualem[1]

Abstract. The paper presents an *a posteriori* error estimator for a (piecewise linear) nonconforming finite element approximation of the heat equation in $\mathbb{R}^d$, $d = 2$ or 3, using backward Euler's scheme. For this discretization, we derive a residual indicator, which use a spatial residual indicator based on the jumps of normal and tangential derivatives of the nonconforming approximation and a time residual indicator based on the jump of broken gradients at each time step. Lower and upper bounds form the main results with minimal assumptions on the mesh. Numerical experiments and a space-time adaptive algorithm confirm the theoretical predictions.

Mathematics Subject Classification. 65N15, 65N30, 65M50.

Received: July 12, 2004.

1. Introduction

This paper deals with the *a posteriori* analysis of the heat equation approximated using backward Euler's scheme in time and a (piecewise linear) nonconforming finite element approximation in space. There are several reasons to use nonconforming approximations. For example the approximation of the Stokes system requires the stability of the method, namely the discrete space has to satisfy the so-called inf-sup condition with a constant independent of the aspect ratio of the elements. Unfortunately standard conforming elements (like the mini element, the Taylor-Hood element, etc.) are not stable on anisotropic meshes (meshes for which the aspect ratio is no more bounded [3] and often used for the approximation of edge singularities and/or boundary layers), see [2, 4] and the references cited there. Therefore the use of nonconforming elements may be recommended since they are unconditionally stable [5].

As a first attempt we consider the case of the heat equation approximated by a piecewise linear nonconforming finite element space based on a regular family of triangulations. However our method may be extended to the Stokes system and to the use of anisotropic meshes. This will be investigated in forthcoming works.

In the conforming case several approaches have been introduced to define error estimators for the heat equation and the Stokes system [6–9, 17, 18, 20, 22]. To be able to extend these techniques to nonconforming spatial approximations, as for elliptic problems [14], we need to be able to estimate the consistency term appearing in the error equation. As in [14], this term is managed using a Helmholtz decomposition of the error. This allows us to extend the results from [7–9, 22] to the nonconforming case.

Keywords and phrases. Error estimator, nonconforming FEM, heat equation.

[1] Université de Valenciennes et du Hainaut Cambrésis, MACS, ISTV, 59313 Valenciennes Cedex 9, France.
Serge.Nicaise@univ-valenciennes.fr; Nadir.Soualem@univ-valenciennes.fr

The schedule of the paper is the following one: Section 2 recalls the continuous and its discretizations. In Section 3 we give some analytical tools, in particular some properties satisfied by the spatial error and its Helmholtz like decomposition. Section 4 is devoted to the *a posteriori* analysis of the time discretization. The efficiency and reliability of the spatial error estimator are established in Section 5. The *a posteriori* analysis of the full discrete problem is considered in Section 6, where we show the efficiency and reliability of the sum of the spatial and time error estimators. Finally in Section 7, we present some numerical tests which confirm our theoretical analysis. We further describe a space-time adaptive algorithm, which is validated by two relevant examples.

2. The continuous, time semi-discrete and full discrete problems

Let Ω be an open bounded of $\mathbb{R}^d$, $d = 2$ or 3, with a polygonal ($d = 2$) or polyhedral ($d = 3$) boundary Γ. For the sake of simplicity, we assume that Ω is simply connected and that its boundary is connected. Let T be a positive and fixed real number.

Let us introduce some notation used in the whole paper: for shortness, if D is a subset of Ω, the $L^2(D)$-norm (resp. $L^2(D)$ inner product) will be denoted by $\|\cdot\|_D$ (resp. $(\cdot,\cdot)_D$). In the case $D = \Omega$, we will drop the index Ω. The usual norm and seminorm of the standard Sobolev space $H^s(D)$, with $s > 0$, are denoted by $\|\cdot\|_{s,D}$ and $|\cdot|_{s,D}$.

In this paper we consider the following heat equation: Let u be the solution of

$$\begin{cases} \dfrac{\partial u}{\partial t} - \Delta u = f \text{ in } \Omega\times]0,T[, \\ u(.,t) = 0 \quad \text{on } \Gamma\times]0,T[, \\ u(.,0) = u_0 \qquad \text{in } \Omega. \end{cases} \tag{1}$$

The datum f is supposed to satisfy $f \in L^2(0,T;H^{-1}(\Omega))$ and the initial value $u_0 \in L^2(\Omega)$. Under these assumptions, problem (1) or equivalently

$$(\partial_t u(t), v) + (\nabla u(t), \nabla v) = (f(t), v), \forall v \in H_0^1(\Omega), \forall \text{ a.e. } t \in (0,T), \tag{2}$$

has a unique (weak) solution in $L^2(0,T;H_0^1(\Omega)) \cap C([0,T];L^2(\Omega))$.

2.1. Time discretization using Euler's scheme

We now suppose that $f \in C([0,T];H^{-1}(\Omega))$. We further introduce a partition of $[0,T]$ into subintervals $[t_{p-1},t_p]$, $1 \le p \le N$ such that $0 = t_0 < t_1 < \cdots < t_N = T$. Denote by $\tau_p = t_p - t_{p-1}$ the length of $[t_{p-1},t_p]$ and by $\tau = \max_p \tau_p$ the global time mesh size.

The semi-discrete approximation of the continuous problem (1) by a backward Euler scheme consists in finding a sequence $(u^p)_{0\le p\le N}$ solution of

$$\begin{cases} \dfrac{u^p - u^{p-1}}{\tau_p} - \Delta u^p = f^p \text{ in } \Omega \quad 1 \le p \le N, \\ u^p = 0 \qquad\qquad\qquad \text{on } \Gamma \quad 1 \le p \le N, \\ u^0 = u_0 \qquad\qquad\qquad \text{in } \Omega, \end{cases} \tag{3}$$

with $f^p = f(\cdot,t_p)$. This problem admits a unique weak solution $u^p \in H_0^1(\Omega)$, whose variational formulation is

$$\int_\Omega u^p v + \tau_p \int_\Omega \nabla u^p \cdot \nabla v = \int_\Omega u^{p-1} v + \tau_p \int_\Omega f^p v \quad \forall v \in H_0^1(\Omega). \tag{4}$$

The unique solvability of the variational formulation (4) is then a direct consequence of the Lax-Milgram lemma.

2.2. **Full discretization**

Problem (4) is now discretized by a nonconforming finite element method. For that purpose, for all $p = 0, 1, \cdots, N$, let us fix a conforming mesh T_{ph} of Ω which form a regular family of triangulations in Ciarlet's sense ([11], p. 124), *i.e.*, there exists $\sigma > 0$ such that

$$h_K/\rho_K \leq \sigma, \forall K \in T_{ph},$$

where we recall that h_K is the diameter of K and ρ_K is the diameter of the largest ball included into K. All elements are triangles or tetrahedra and will be denoted by K. For all p, we denote by $h_p = \max_{K \in T_{ph}} h_K$. The set of all edges/faces of T_{ph} is denoted by $\mathcal{E}_{ph}$. Let $\mathcal{E}_{ph}^{int}$ be the set of interior edges/faces of T_{ph} and $\mathcal{E}_K$ be the set of the edges/faces of the element K. Finally for an edge/face $E \in \mathcal{E}_K \cap \mathcal{E}_L$ we denote by $h_E = \frac{1}{2}(\frac{d|K|}{|E|} + \frac{d|L|}{|E|})$, its mean height.

Introduce the Crouzeix-Raviart nonconforming finite element space:

$$\begin{aligned} X_{ph}^0 = \{ & v \in L^2(\Omega) : v_{|K} \in \mathbb{P}_1, \forall K \in T_{ph}, \\ & \int_E v_{|K} = \int_E v_{|L}, \forall E \in \mathcal{E}_K \cap \mathcal{E}_L \cap \mathcal{E}_{ph}^{int}, K, L \in T_{ph}, \\ & \int_E v_{|K} = 0, \forall E \in \mathcal{E}_K \cap \Gamma, K \in T_{ph}\}. \end{aligned}$$

The full discrete approximation of problem (1) using Euler's scheme and the Crouzeix-Raviart nonconforming finite element, is then given by: given an approximation $u_h^0 \in X_{0h}^0$ of u_0, find $u_h^p \in X_{ph}^0$, $1 \leq p \leq N$, such that:

$$\int_\Omega u_h^p v_h + \tau_p \sum_{K \in T_{ph}} \int_K \nabla u_h^p \nabla v_h = \int_\Omega u_h^{p-1} v_h + \tau_p \int_\Omega f^p v_h \tag{5}$$

for all $v_h \in X_{ph}^0$.

Note that the Crouzeix-Raviart elements were recently used in [1] for the discretization of a mixed formulation of the Laplace equation and that the nonconformity of the approximation also renders their *a posteriori* analysis more delicate.

Definition 2.1. Let u^p be a solution of (4) and u_h^p a solution of (5), then we denote the spatial error by

$$e^p = u^p - u_h^p.$$

Let us finish this section by introducing some useful notation and properties used below.

The notation $a \lesssim b$ and $a \sim b$ means the existence of positive constants C_1 and C_2 (which are independent of the mesh size of the triangulations, of the time step size and of the function under consideration) such that $a \leq C_2 b$ and $C_1 b \leq a \leq C_2 b$, respectively.

For a boundary edge/face E we denote the outward normal vector by n_E. In 2D, we further define the tangent vector by $t_E = (-n_{E2}, n_{E1})$ if $n_E = (n_{E1}, n_{E2})$. Given an interior edge/face E, we choose an arbitrary normal direction n_E and denote by K_{in} and K_{ext} the two elements sharing this edge/face. Without any restriction, we may suppose here that n_E is pointing to K_{ext} like in Figure 1. In 2D, denote as before the tangent vector by $t_E = (-n_{E2}, n_{E1})$ if $n_E = (n_{E1}, n_{E2})$.

For the analysis of the nonconforming approximation, we will use the following Crouzeix-Raviart property:

$$\int_E [\![u_h]\!]_E = 0 \qquad \forall E \in \mathcal{E}_{ph}, \forall u_h \in X_{ph}^0, \tag{6}$$

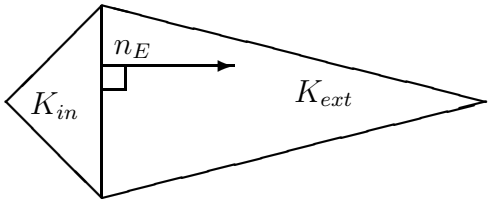

FIGURE 1. Two elements sharing the edge E.

where the jump of some function v across an edge/face E at a point x is defined by

$$[\![v(x)]\!]_E = \begin{cases} \lim\limits_{\alpha\to 0^+} v(x+\alpha n_E) - v(x-\alpha n_E) & \text{if } E \in \mathcal{E}_{ph}^{int}, \\ v(x) & \text{if } E \in \mathcal{E}_{ph} \setminus \mathcal{E}_{ph}^{int}. \end{cases}$$

Note that the sign of $[\![v(x)]\!]_E$ depends on the orientation of n_E. However, quantity like a gradient jump $[\![\nabla v \cdot n_E]\!]_E$ is independent of this orientation.

For a function $v \in X_{ph}^0$ we define its broken gradient $\nabla_h v$ by

$$(\nabla_h v)_{|K} = \nabla(v_{|K}), \forall K \in T_{ph}.$$

In the sequel we will use local patches: for an element K we define ω_K as the union of all elements having a common edge/face with K, for an edge/face E, let ω_E be the union of both elements having E as edge/face and finally for a node x, let ω_x be the union of both elements having x as node. Similarly denote by $\tilde{\omega}_K$ (resp. $\tilde{\omega}_E$) the union of all triangles sharing a node with K (resp. E).

We further need the standard $\mathbb{P}_1$ conforming finite element spaces

$$\begin{aligned} V_{ph} &= \{v \in H^1(\Omega) : v_{|K} \in \mathbb{P}_1, \forall K \in T_{ph}\}, \\ V_{ph}^0 &= V_{ph} \cap H_0^1(\Omega). \end{aligned}$$

For our error analysis we require an interpolant that maps $X_{ph}^0 \oplus H_0^1(\Omega)$ to V_{ph}^0. Hence Lagrange interpolation operator is unsuitable but Clément like interpolation operator is more appropriate. To write the results in the largest setting as possible, let us set

$$\begin{aligned} Y_{ph} = \{&v \in L^2(\Omega) : v_{|K} \in H^1(K), \forall K \in T_{ph}, \\ &\int_E v_{|K} = \int_E v_{|L}, \forall E \in \mathcal{E}_K \cap \mathcal{E}_L \cap \mathcal{E}_{ph}^{int}, K, L \in T_{ph}, \}, \\ Y_{ph}^0 = \{&v \in L^2(\Omega) : v_{|K} \in H^1(K), \forall K \in T_{ph}, \\ &\int_E v_{|K} = \int_E v_{|L}, \forall E \in \mathcal{E}_K \cap \mathcal{E}_L \cap \mathcal{E}_{ph}^{int}, K, L \in T_{ph}, \\ &\int_E v_{|K} = 0, \forall E \in \mathcal{E}_K \cap \Gamma, K \in T_{ph}\}. \end{aligned}$$

Note that $H^1(\Omega) \subset Y_{ph}$ and that $X_{ph}^0 \oplus H_0^1(\Omega) \subset Y_{ph}^0$.

Recall that the Clément interpolation operator is defined as follows: Denote by $\mathcal{N}_{ph}$ the set of nodes of the triangulation T_{ph} and by $\mathcal{N}_{ph}^{int}$ the set of interior nodes of the triangulation T_{ph}. For each node x denote further by λ_x the standard hat function associated with x, namely $\lambda_x \in V_{ph}$ and satisfies

$$\lambda_x(y) = \delta_{x,y}, \forall y \in \mathcal{N}_{ph}.$$

For any $v \in Y_{ph}$ and $w \in Y_{ph}^0$, we define $I_C v$ and $I_C^0 w$ by

$$I_C v = \sum_{x \in \mathcal{N}_{ph}} |\omega_x|^{-1} \left(\int_{\omega_x} v \right) \lambda_x, \tag{7}$$

$$I_C^0 w = \sum_{x \in \mathcal{N}_{ph}^{int}} |\omega_x|^{-1} \left(\int_{\omega_x} w \right) \lambda_x. \tag{8}$$

Note that $I_C v$ belongs to V_{ph}, while $I_C^0 w$ belongs to V_{ph}^0. Moreover these operators have the following properties:

Lemma 2.2. *For all $v \in Y_{ph}$ and $w \in Y_{ph}^0$, we have*

$$\|v - I_C v\|_K \lesssim h_K \|\nabla_h v\|_{\tilde{\omega}_K}, \forall K \in T_{ph}, \tag{9}$$

$$\|v - I_C v\|_E \lesssim h_E^{1/2} \|\nabla_h v\|_{\tilde{\omega}_E}, \forall E \in \mathcal{E}_{ph}, \tag{10}$$

$$\left\|w - I_C^0 w\right\|_K \lesssim h_K \|\nabla_h w\|_{\tilde{\omega}_K}, \forall K \in T_{ph}, \tag{11}$$

$$\|w - I_C^0 w\|_E \lesssim h_E^{1/2} \|\nabla_h w\|_{\tilde{\omega}_E}, \forall E \in \mathcal{E}_{ph}^{int}, \tag{12}$$

$$\|\nabla I_C^0 w\|_K \lesssim \|\nabla_h w\|_{\tilde{\omega}_K}, \forall K \in T_{ph}. \tag{13}$$

Proof. For v and w in $H^1(\Omega)$, the above properties are proved in [12] (see also [19, 21] for other interpolation operators) using scaling arguments, but a careful analysis of their proof reveals that these properties hold for v and w as in the statement of the Lemma. □

The mean value of some function v on an edge/face E is defined by

$$\mathcal{M}_E(v) = \frac{1}{|E|} \int_E v.$$

In the sequel we often need the following Green's formulas: if D is a bounded open subset of $\mathbb{R}^2$ and $v, w \in H^1(D)$, then we have

$$\int_D \nabla v \cdot \boldsymbol{curl}\ w = \int_{\partial D} v \boldsymbol{curl}\ w \cdot n = \int_{\partial D} \nabla v \cdot t w, \tag{14}$$

where t is the unit tangent vector along ∂D and $\boldsymbol{curl}\ w$ is the vectorial curl of w, namely $\boldsymbol{curl}\ w = \begin{pmatrix} \partial_2 w \\ -\partial_1 w \end{pmatrix}$.

Similarly if D is a bounded open subset of $\mathbb{R}^3$ and $v \in H^1(D)$, $w \in H^1(D)^3$ then we have

$$\int_D \nabla v \cdot \boldsymbol{curl}\ w = \int_{\partial D} v \boldsymbol{curl}\ w \cdot n = \int_{\partial D} (\nabla v \times n) \cdot w. \tag{15}$$

We finally introduce the gradient jump of u_h^p in normal and tangential direction by

$$J_{E,n}^p = \begin{cases} \left[\!\left[\nabla u_h^p \cdot n_E\right]\!\right]_E & \text{if } E \in \mathcal{E}_{ph}^{int}, \\ 0 & \text{if } E \in \mathcal{E}_{ph} \setminus \mathcal{E}_{ph}^{int}. \end{cases}$$

If $d = 2$, then

$$J_{E,t}^p = \begin{cases} \left[\!\left[\nabla u_h^p \cdot t_E\right]\!\right]_E & \text{if } E \in \mathcal{E}_{ph}^{int}, \\ -\nabla u_h^p \cdot t_E & \text{if } E \in \mathcal{E}_{ph} \setminus \mathcal{E}_{ph}^{int}. \end{cases}$$

If $d = 3$, then

$$J_{E,t}^p = \begin{cases} \left[\!\left[\nabla u_h^p \times n_E\right]\!\right]_E & \text{if } E \in \mathcal{E}_{ph}^{int}, \\ -\nabla u_h^p \times n_E & \text{if } E \in \mathcal{E}_{ph} \setminus \mathcal{E}_{ph}^{int}. \end{cases}$$

3. Some analytical tools

In this section we collect different properties satisfied by the spatial error e^p that we will use in the proof of the spatial error bounds.

Lemma 3.1 (Galerkin orthogonality)**.** *The error e^p satisfies the Galerkin orthogonality relation*

$$\sum_{K\in T_{ph}}\int_K \nabla_h e^p\cdot\nabla v_h=\int_\Omega \frac{e^{p-1}-e^p}{\tau_p}v_h, \forall v_h\in V_{ph}^0. \tag{16}$$

Proof. It suffices to subtract (4) with $v=v_h\in V_{ph}^0$ to the identity (5). □

Lemma 3.2. *Let $\varphi\in H^1(\Omega)$ if $d=2$ and $\varphi\in H^1(\Omega)^3$ if $d=3$. Then the error satisfies the following identity*

$$\int_\Omega \nabla_h e^p\cdot \boldsymbol{curl}\ \varphi=\sum_{E\in\mathcal{E}_{ph}}\int_E J_{E,t}^p\cdot\varphi. \tag{17}$$

Proof. Assume that $d=2$. Integrations by parts in Ω and in each element K give (see (14))

$$\begin{aligned}\int_\Omega \nabla_h e^p\cdot \boldsymbol{curl}\ \varphi &= \int_\Omega \nabla u^p\cdot \boldsymbol{curl}\ \varphi-\sum_{K\in T_{ph}}\int_K \nabla u_h^p\cdot \boldsymbol{curl}\ \varphi\\ &=\int_\Gamma \boldsymbol{curl}\ \varphi\cdot n u^p-\sum_{K\in T_{ph}}\int_{\partial K}\nabla u_h^p\cdot t_K\varphi.\end{aligned}$$

As $u^p\in H_0^1(\Omega)$ and $\varphi\in H^1(\Omega)$, we conclude using the definition of $J_{E,t}^p$.

The proof is similar in dimension 3 using (15). □

Lemma 3.3 (error orthogonality)**.** *The error satisfies*

$$\sum_{K\in T_{ph}}\int_K \nabla_h e^p\cdot \boldsymbol{curl}\ \varphi_h=0, \forall\varphi_h\in V_{ph}\ \text{ if } d=2 \text{ and } \varphi_h\in (V_{ph})^3 \text{ if } d=3. \tag{18}$$

Proof. Consider an arbitrary element φ_h in V_{ph} if $d=2$ or in $(V_{ph})^3$ if $d=3$. As before, by integrating by parts (*cf.* the identities (14) and (15)), we obtain (recalling that $u^p\in H_0^1(\Omega)$)

$$\begin{aligned}\sum_{K\in T_{ph}}\int_K \nabla_h e^p\cdot \boldsymbol{curl}\ \varphi_h &= \int_\Omega \nabla u^p\cdot \boldsymbol{curl}\ \varphi_h-\sum_{K\in T_{ph}}\int_K \nabla_h u_h^p\cdot \boldsymbol{curl}\ \varphi_h\\ &=\int_\Gamma u^p \boldsymbol{curl}\ \varphi_h\cdot n-\sum_{K\in T_{ph}}\int_{\partial K} u_h^p \boldsymbol{curl}\ \varphi_h\cdot n_K\\ &=-\sum_{K\in T_{ph}}\int_{\partial K} u_h^p \boldsymbol{curl}\ \varphi_h\cdot n_K\\ &=-\sum_{E\in\mathcal{E}_{ph}}\int_E \left[\!\left[u_h^p\right]\!\right]_E \boldsymbol{curl}\ \varphi_h\cdot n_E\\ &=-\sum_{E\in\mathcal{E}_{ph}}(\boldsymbol{curl}\ \varphi_h\cdot n_E)\int_E \left[\!\left[u_h^p\right]\!\right]_E,\end{aligned}$$

since the function $(\boldsymbol{curl}\ \varphi_h\cdot n_E)|_E$ is constant on $E\in\mathcal{E}_{ph}$. The Crouzeix-Raviart property (6) satisfied by $u_h^p\in X_{ph}^0$ allows us to finish the proof. □

Lemma 3.4. *The error e^p satisfies*

$$\sum_{K\in T_{ph}}\int_K \nabla_h e^p\cdot\nabla w = \sum_{K\in T_{ph}}\int_K\left(f^p-\frac{u^p-u^{p-1}}{\tau_p}\right)w+\sum_{E\in\mathcal{E}_{ph}}\int_E J^p_{E,n}w,$$

for any $w\in H^1_0(\Omega)$.

Proof. Elementwise integration by parts and the observation that $\Delta u^p_h=0$ on all $K\in T_{ph}$ yield

$$\begin{aligned}\sum_{K\in T_{ph}}\int_K \nabla_h e^p\nabla w &= \int_\Omega \nabla u^p\cdot\nabla w-\sum_{K\in T_{ph}}\int_K\nabla_h u^p_h\cdot\nabla w\\ &=\int_\Omega\left(f^p-\frac{u^p-u^{p-1}}{\tau_p}\right)w\\ &\quad-\sum_{K\in T_{ph}}\left(-\int_K\Delta u^p_h w+\int_{\partial K} n\cdot\nabla u^p_h w\right)\\ &=\int_\Omega\left(f^p-\frac{u^p-u^{p-1}}{\tau_p}\right)w\\ &\quad-\sum_{K\in T_{ph}}\sum_{E\in\mathcal{E}_K}\int_E n\cdot\nabla u^p_h w.\end{aligned}$$

We conclude by using the definition of $J^p_{E,n}$ and the continuity of w through the edges/faces. □

Corollary 3.5. *For any $w\in H^1_0(\Omega)$ and $\varphi\in H^1(\Omega)$ if $d=2$ and $\varphi\in H^1(\Omega)^3$ if $d=3$, we have*

$$\sum_{K\in T_{ph}}\int_K\nabla_h e^p\cdot(\nabla w+\boldsymbol{curl}\,\varphi)=\sum_{K\in T_{ph}}\int_K\left(f^p-\frac{u^p-u^{p-1}}{\tau_p}\right)w+\sum_{E\in\mathcal{E}_{ph}}\int_E(J^p_{E,n}w+J^p_{E,t}\cdot\varphi). \tag{19}$$

Proof. Direct consequence of Lemmas 3.2 and 3.4. □

We now recall the following result (see Lem. 3.2 of [14] in 2D and [13] in 3D or [15], Chap. I):

Lemma 3.6 (Helmholtz decomposition of the error)**.** *We have the following error decomposition*

$$\nabla_h e^p=\nabla w^p+\boldsymbol{curl}\,\varphi^p, \tag{20}$$

with $\varphi^p\in H^1(\Omega)$ if $d=2$ and $\varphi^p\in(H^1(\Omega))^3$ if $d=3$ and $w^p\in H^1_0(\Omega)$. Moreover the next estimates hold:

$$|w^p|_{1,\Omega}\le\|\nabla_h e^p\|, \tag{21}$$

$$|\varphi^p|_{1,\Omega}\lesssim\|\nabla_h e^p\|. \tag{22}$$

Proof. We consider the following Dirichlet problem: find $w^p\in H^1_0(\Omega)$ solution of

$$\begin{cases}\boldsymbol{div}\,(\nabla_h e^p-\nabla w^p)=0 \text{ in }\Omega,\\ w^p=0 \qquad\qquad\qquad\quad \text{on }\Gamma.\end{cases} \tag{23}$$

The weak formulation of that problem (23) is:

$$\int_\Omega\nabla w^p\cdot\nabla v=\int_\Omega\nabla_h e^p\cdot\nabla v,\quad\forall v\in H^1_0(\Omega). \tag{24}$$

As the vector field $\nabla_h e^p - \nabla w^p$ is divergence free in Ω, *i.e.*,

$$\boldsymbol{div}\ (\nabla_h e^p - \nabla w^p) = 0 \text{ in } \Omega.$$

By Theorem I.3.1 of [15] if $d = 2$ or Theorem I.3.4 of [15] if $d = 3$, there exists $\varphi^p \in H^1(\Omega)$ if $d = 2$ and $\varphi^p \in (H^1(\Omega))^3$ if $d = 3$ such that

$$\boldsymbol{curl}\ \varphi^p = \nabla_h e^p - \nabla w^p.$$

The estimate (21) directly follows by using (24) with $v = w^p$. The second estimate (22) is obtained as follows. Using the expansion (20), we may write

$$\begin{aligned}\int_\Omega |\boldsymbol{curl}\ \varphi^p|^2 &= \int_\Omega \boldsymbol{curl}\ \varphi^p \cdot \boldsymbol{curl}\ \varphi^p \\ &= \int_\Omega \boldsymbol{curl}\ \varphi^p \cdot (\nabla_h e^p - \nabla w^p).\end{aligned}$$

By Green's formula and the boundary conditions $w^p = 0$ on Γ, we obtain

$$\int_\Omega |\boldsymbol{curl}\ \varphi^p|^2 = \int_\Omega \boldsymbol{curl}\ \varphi^p \cdot \nabla_h e^p. \tag{25}$$

By Cauchy-Schwarz's inequality we conclude

$$\|\boldsymbol{curl}\ \varphi^p\| \leq \|\nabla_h e^p\|. \tag{26}$$

If $d = 2$ the estimate (22) directly follows from the above estimate since $|\varphi^p|_{1,\Omega} = \|\boldsymbol{curl}\ \varphi^p\|$. If $d = 3$, we may notice that the application of the closed graph theorem yields a vector field φ^p satisfying

$$\|\varphi^p\|_{1,\Omega} \lesssim \|\boldsymbol{curl}\ \varphi^p\|. \tag{27}$$

Indeed it suffices to consider the mapping

$$F : H^1(\Omega)^3/K \to \{w \in L^2(\Omega)^3 : \boldsymbol{div}\ w = 0\} : \varphi \to \boldsymbol{curl}\ \varphi,$$

where $K = \{\varphi \in H^1(\Omega)^3 : \boldsymbol{curl}\ \varphi = 0\}$. This mapping is continuous and bijective (by Thm. I.3.4 of [15]) and consequently by the closed graph theorem, its inverse mapping is also continuous.

Therefore we may conclude as before using the above estimates (26) and (27). □

The above lemmas allow us to prove the

Lemma 3.7. *The following identities hold*

$$\tau_p \int_\Omega \nabla_h e^p \cdot \nabla w^p = \tau_p \int_\Omega \left(f^p - \frac{u_h^p - u_h^{p-1}}{\tau_p} \right) (w^p - I_C^0 w^p) + \tau_p \sum_{E \in \mathcal{E}_{ph}} \int_E J_{E,n}^p (w^p - I_C^0 w^p) - \int_\Omega (e^p - e^{p-1}) w^p, \tag{28}$$

$$\int_\Omega \nabla_h e^p \cdot \boldsymbol{curl}\ \varphi^p = \sum_{E \in \mathcal{E}_{ph}} \int_E J_{E,t}^p \cdot (\varphi^p - I_C \varphi^p), \tag{29}$$

$$\begin{aligned} \|e^p\|^2 + \tau_p \int_\Omega |\nabla_h e^p|^2 = {} & (e^{p-1}, e^p) + (e^p - e^{p-1}, e^p - w^p - I_C^0(e^p - w^p)) \\ & + \tau_p \int_\Omega \nabla_h e^p \cdot \nabla I_C^0 (e^p - w^p) + \tau_p \int_\Omega \left(f^p - \frac{u_h^p - u_h^{p-1}}{\tau_p} \right) (w^p - I_C^0 w^p) \\ & + \tau_p \sum_{E \in \mathcal{E}_{ph}} \int_E (J_{E,n}^p (w^p - I_C^0 w^p) + J_{E,t}^p \cdot (\varphi^p - I_C \varphi^p)). \end{aligned} \tag{30}$$

Proof. The identity (28) follows from the Galerkin relation of Lemma 3.1 with $v_h = I_C^0 w^p \in V_{ph}^0$ and Lemma 3.4. The second identity (29) is a consequence of the orthogonality relation of Lemma 3.3 with $\varphi_h = I_C \varphi^p$ and Lemma 3.2.

Using the error decomposition (20) we may write

$$\tau_p \int_\Omega |\nabla_h e^p|^2 = \tau_p \int_\Omega \nabla_h e^p \cdot (\nabla w^p + \boldsymbol{curl}\ \varphi^p).$$

Therefore the identities (28), (29) directly lead to

$$\begin{aligned} \tau_p \int_\Omega |\nabla_h e^p|^2 = {} & - \int_\Omega (e^p - e^{p-1}) w^p + \tau_p \int_\Omega \left(f^p - \frac{u_h^p - u_h^{p-1}}{\tau_p} \right) (w^p - I_C^0 w^p) \\ & + \tau_p \sum_{E \in \mathcal{E}_{ph}} \int_E (J_{E,n}^p (w^p - I_C^0 w^p) + J_{E,t}^p \cdot (\varphi^p - I_C \varphi^p)). \end{aligned}$$

This identity may be equivalently written

$$\begin{aligned} \|e^p\|^2 + \tau_p \int_\Omega |\nabla_h e^p|^2 = {} & (e^{p-1}, e^p) + (e^p - e^{p-1}, e^p - w^p - I_C^0(e^p - w^p)) + (e^p - e^{p-1}, I_C^0(e^p - w^p)) \\ & + \tau_p \int_\Omega \left(f^p - \frac{u_h^p - u_h^{p-1}}{\tau_p} \right) (w^p - I_C^0 w^p) \\ & + \tau_p \sum_{E \in \mathcal{E}_{ph}} \int_E (J_{E,n}^p (w^p - I_C^0 w^p) + J_{E,t}^p \cdot (\varphi^p - I_C \varphi^p)). \end{aligned}$$

This identity and the Galerkin orthogonality relation (16) lead to (30). □

4. *A POSTERIORI* ANALYSIS OF THE TIME DISCRETIZATION

Inspired from [7, 9, 16, 17], we define the time error indicators:

$$\eta_t^p = \tau_p^{1/2} \|\nabla_h (u_h^p - u_h^{p-1})\|, 1 \le p \le N. \tag{31}$$

The only difference with the above papers relies on the fact that $u_h^p - u_h^{p-1}$ is not in $H^1(\Omega)$. Since the continuous problems (2) and (4) are not related to the approximation spaces X_{ph}^0, we easily adapt the arguments used there to our setting.

Note that in (31) we have written $\nabla_h(u_h^p - u_h^{p-1})$ while u_h^p and u_h^{p-1} are not related to the same triangulation, but $u_h^p - u_h^{p-1}$ may be seen as a piecewise $\mathbb{P}_1$-function on the "triangulation" $T_{ph} \cap T_{p-1,h}$ made of the intersections of elements from T_{ph} with elements from $T_{p-1,h}$. The broken gradient is then calculated on this triangulation $T_{ph} \cap T_{p-1,h}$.

For shortness we introduce the following notation: Denote by $\pi_\tau f$ the step function which is constant and equal to $f(t_p)$ on each interval (t_{p-1}, t_p), $1 \le p \le N$. For a sequence $v^p \in X_{ph}^0 \oplus H_0^1(\Omega)$, $0 \le p \le N$, we denote by v_τ its "Lagrange" interpolant, which is affine on each interval $[t_{p-1}, t_p]$, $1 \le p \le N$, and equal to v^p at t_p, *i.e.*, defined by,

$$v_\tau(t) = \frac{t_p - t}{\tau_p} v^{p-1} + \frac{t - t_{p-1}}{\tau_p} v^p, \forall t \in [t_{p-1}, t_p], 1 \le p \le N.$$

Denote finally $e_\tau = u - u_\tau$, the time discretization error.

As

$$\partial_t u_\tau = \frac{u^p - u^{p-1}}{\tau_p} \text{ on } (t_{p-1}, t_p),$$

the semi-discrete equation (4) is equivalent to

$$(\partial_t u_\tau(t), v) + (\nabla u^p, \nabla v) = (f^p, v), \forall v \in H_0^1(\Omega), \forall t \in (t_{p-1}, t_p). \tag{32}$$

Taking the difference with (2), we derive the residual equation

$$(\partial_t e_\tau(t), v) + (\nabla e_\tau(t), \nabla v) = ((f - f^p)(t), v) + (\nabla(u^p - u_\tau)(t), \nabla v), \forall v \in H_0^1(\Omega), \forall a.e.\ t \in (t_{p-1}, t_p). \tag{33}$$

This equation allows to prove the

Theorem 4.1 (time upper error bound)**.** *The next estimate holds*

$$\|e_\tau(t_n)\|^2 + \int_0^{t_n} \|\nabla e_\tau(s)\|^2 \, \mathrm{d}s \lesssim \sum_{p=1}^{n} (\eta_t^p)^2 + \int_0^{t_n} \|\nabla_h(u_\tau - u_{h\tau})(s)\|^2 \, \mathrm{d}s + \|f - \pi_\tau f\|^2_{L^2(0,t_n;H^{-1}(\Omega))}. \tag{34}$$

Proof. The residual equation (33) yields (see Prop. 3.1 of [9])

$$\|e_\tau(t_n)\|^2 + \int_0^{t_n} \|\nabla e_\tau(t)\|^2 \, \mathrm{d}t \le 2 \sum_{p=1}^{n} \int_{t_{p-1}}^{t_p} \|\nabla(u^p - u_\tau)(s)\|^2 \, \mathrm{d}s + 2\|f - \pi_\tau f\|^2_{L^2(0,t_n;H^{-1}(\Omega))}. \tag{35}$$

By the definition of u_τ we clearly have

$$\int_{t_{p-1}}^{t_p} \|\nabla(u^p - u_\tau)(s)\|^2 \, \mathrm{d}s = \frac{\tau_p}{3} \|\nabla(u^p - u^{p-1})\|^2. \tag{36}$$

Using the triangular inequality, we simply write

$$\tau_p^{1/2} \|\nabla(u^p - u^{p-1})\| \le \eta_t^p + \tau_p^{1/2} \|\nabla_h(u^p - u_h^p)\| + \tau_p^{1/2} \|\nabla_h(u_h^{p-1} - u_h^{p-1})\|.$$

Moreover the arguments from Lemma 2.3 of [9] yields

$$\tau_p \|\nabla_h(u^p - u_h^p)\|^2 + \tau_p \|\nabla_h(u_h^{p-1} - u_h^{p-1})\|^2 \lesssim \int_{t_{p-1}}^{t_p} \|\nabla_h(u_\tau - u_{h\tau})(s)\|^2 \, \mathrm{d}s. \tag{37}$$

The above identity and these two estimates yield

$$\int_{t_{p-1}}^{t_p} \|\nabla(u^p - u_\tau)(s)\|^2 \,\mathrm{d}s \lesssim (\eta_t^p)^2 + \int_{t_{p-1}}^{t_p} \|\nabla_h(u_\tau - u_{h\tau})(s)\|^2 \,\mathrm{d}s. \tag{38}$$

This estimate in (35) leads to the conclusion. □

Corollary 4.2 (second time upper error bound)**.** *The next estimate holds*

$$\|\partial_t e_\tau\|^2_{L^2(0,t_n;H^{-1}(\Omega))} \lesssim \sum_{p=1}^{n} (\eta_t^p)^2 + \int_0^{t_n} \|\nabla_h(u_\tau - u_{h\tau})(s)\|^2 \,\mathrm{d}s + \|f - \pi_\tau f\|^2_{L^2(0,t_n;H^{-1}(\Omega))}. \tag{39}$$

Proof. The residual equation (33) directly gives

$$\|\partial_t e_\tau\|^2_{L^2(0,t_n;H^{-1}(\Omega))} \lesssim \|f - \pi_\tau f\|^2_{L^2(0,t_n;H^{-1}(\Omega))} + \int_0^{t_n} \|\nabla e_\tau(s)\|^2 \,\mathrm{d}s + \sum_{p=1}^{n} \int_{t_{p-1}}^{t_p} \|\nabla(u^p - u_\tau)(s)\|^2 \,\mathrm{d}s.$$

The second term of this right-hand side is estimated in (34), while the third term is estimated *via* (38). □

The local time upper bound is even easier to prove:

Theorem 4.3 (time lower error bound)**.** *For all $p = 1, \cdots, N$, the next estimate holds*

$$\begin{aligned}\eta_t^p \lesssim{}& \|\nabla_h e_\tau\|_{L^2(t_{p-1},t_p;L^2(\Omega))} + \|\partial_t e_\tau\|_{L^2(t_{p-1},t_p;H^{-1}(\Omega))} \\ &+ \tau_p^{1/2}(\|\nabla_h(u^p - u_h^p)\| + \|\nabla_h(u^{p-1} - u_h^{p-1})\|) + \|f - \pi_\tau f\|_{L^2(t_{p-1},t_p;H^{-1}(\Omega))}.\end{aligned} \tag{40}$$

Proof. By the triangular inequality we may write

$$\eta_t^p \lesssim \tau_p^{1/2}(\|\nabla(u^p - u^{p-1})\| + \|\nabla_h(u^p - u_h^p)\| + \|\nabla_h(u^{p-1} - u_h^{p-1})\|).$$

The estimation of the term $\tau_p^{1/2}\|\nabla(u^p - u^{p-1})\|$ is made as in Proposition 3.3 of [9] by using the identity (36) (with $n = p$) and taking $v = u^p - u_\tau$ in (33) and integrating the result in $t \in (t_{p-1}, t_p)$. □

5. *A POSTERIORI* ANALYSIS OF THE SPATIAL DISCRETIZATION

5.1. Upper error bound

The exact element residual is given by

$$f^p - \frac{u_h^p - u_h^{p-1}}{\tau_p}.$$

As usual [20] it is replaced by an approximate element residual

$$f_h^p - \frac{u_h^p - u_h^{p-1}}{\tau_p},$$

where f_h^p is a finite dimensional approximation of f^p (for instance $(f_h^p)_{|K} := \frac{1}{|K|}\int_K f^p$, for all $K \in T_{ph}$).

Definition 5.1. Let $p \geq 1$. The local error estimator η_K^p is defined by

$$\eta_K^p = h_K \left\| f_h^p - \frac{u_h^p - u_h^{p-1}}{\tau_p} \right\|_K + \sum_{E \in \mathcal{E}_K} h_E^{1/2} \left(\left\| J_{E,n}^p \right\|_E + \left\| J_{E,t}^p \right\|_E \right).$$

The global spatial error estimator η^p is given by

$$(\eta^p)^2 = \sum_{K\in T_{ph}} (\eta_K^p)^2.$$

The local and global approximation terms are defined by

$$\xi_K^p = h_K \left\| f^p - f_h^p \right\|_{\omega_K}, \quad (\xi^p)^2 = \sum_{K\in T_{ph}} (\xi_K^p)^2.$$

Theorem 5.2 (upper error bound)**.** *The next estimate holds*

$$\left\|e^n\right\|^2 + \sum_{p=1}^n \tau_p \left\|\nabla_h e^p\right\|^2 \lesssim \sum_{p=1}^n \max\{h_p^2, \tau_p\}(\eta^p)^2 + \left\|e^0\right\|^2 + \sum_{p=1}^n \tau_p (\xi^p)^2. \tag{41}$$

Proof. This upper bound is a consequence of Lemmas 3.6 and 3.7. We first estimate some terms of the right-hand side of the identity (30) of Lemma 3.7. Using successively Cauchy-Schwarz's inequality, the estimate (11) and the definition 5.1 of the local estimator, we obtain

$$\begin{aligned}\sum_{K\in T_{ph}} \int_K \left(f_h^p - \frac{u_h^p - u_h^{p-1}}{\tau_p} \right) (w^p - I_C^0 w^p) &\lesssim \sum_{K\in T_{ph}} h_K \left\| f_h^p - \frac{u_h^p - u_h^{p-1}}{\tau_p} \right\|_K |w^p|_{1,\tilde{\omega}_K} \\ &\lesssim \sum_{K\in T_{ph}} \eta_K^p \, |w^p|_{1,\tilde{\omega}_K}.\end{aligned}$$

By discrete Cauchy-Schwarz's inequality we get

$$\sum_{K\in T_{ph}} \int_K \left(f_h^p - \frac{u_h^p - u_h^{p-1}}{\tau_p} \right) (w^p - I_C^0 w^p) \lesssim \eta^p \, |w^p|_{1,\Omega}. \tag{42}$$

Similarly using (12) and (10) we estimate the term with the jumps of normal and tangential derivatives:

$$\begin{aligned}\sum_{E\in\mathcal{E}_{ph}} \int_E J_{E,n}^p (w^p - I_C^0 w^p) &\le \sum_{E\in\mathcal{E}_{ph}} \left\| J_{E,n}^p \right\|_E \left\| w^p - I_C^0 w^p \right\|_E \\ &\lesssim \sum_{E\in\mathcal{E}_{ph}} \left\| J_{E,n}^p \right\|_E h_E^{1/2} \, |w^p|_{1,\tilde{\omega}_E} \\ &\lesssim \sum_{K\in T_{ph}} \eta_K^p \, |w^p|_{1,\tilde{\omega}_K}, \\ \sum_{E\in\mathcal{E}_{ph}} \int_E J_{E,t}^p \cdot (\varphi^p - I_C \varphi^p) &\le \sum_{E\in\mathcal{E}_{ph}} \left\| J_{E,t}^p \right\|_E \left\| \varphi^p - I_C \varphi^p \right\|_E \\ &\lesssim \sum_{E\in\mathcal{E}_{ph}} \left\| J_{E,t}^p \right\|_E h_E^{1/2} \, |\varphi^p|_{1,\tilde{\omega}_E} \\ &\lesssim \sum_{K\in T_{ph}} \eta_K^p \, |\varphi^p|_{1,\tilde{\omega}_K}.\end{aligned}$$

As before discrete Cauchy-Schwarz's inequality yields

$$\sum_{E\in\mathcal{E}_{ph}}\int_E J^p_{E,n}(w^p - I^0_C w^p) \lesssim \eta^p \left|w^p\right|_{1,\Omega}, \tag{43}$$

$$\sum_{E\in\mathcal{E}_{ph}}\int_E J^p_{E,t}\cdot(\varphi^p - I_C\varphi^p) \lesssim \eta^p \left|\varphi^p\right|_{1,\Omega}. \tag{44}$$

Again (11) allows to estimate the term:

$$\sum_{K\in T_{ph}}\int_K (f^p - f^p_h)(w^p - I^0_C w^p) \le \sum_{K\in T_{ph}} h_K \left\|f^p - f^p_h\right\|_K \left|w^p\right|_{1,\tilde{\omega}_K},$$

and consequently

$$\sum_{K\in T_{ph}}\int_K (f^p - f^p_h)(w^p - I^0_C w^p) \lesssim \xi^p \left|w^p\right|_{1,\Omega}. \tag{45}$$

Applying Cauchy-Schwarz's inequality and the estimate (11) we get

$$|(e^p - e^{p-1}, e^p - w^p - I^0_C(e^p - w^p))| \lesssim h_p\|e^p - e^{p-1}\|\|\nabla_h(e^p - w^p)\|.$$

The above estimates and (13) in the identity (30) yield

$$\begin{aligned}\|e^p\|^2 + \tau_p\int_\Omega|\nabla_h e^p|^2 \le{}& (e^{p-1}, e^p) + Ch_p\|e^p - e^{p-1}\|\|\nabla_h(e^p - w^p)\| \\ &+C\tau_p\|\nabla_h e^p\|\|\nabla_h(e^p - w^p)\| + C\tau_p\eta^p\left|\varphi^p\right|_{1,\Omega} + C\tau_p(\eta^p + \xi^p)\left|w^p\right|_{1,\Omega},\end{aligned} \tag{46}$$

for some constant $C > 0$ depending only on the minimal angle of T_{ph}.

This estimate does not directly yield the desired estimate due to the factors $\|\nabla_h(e^p - w^p)\|$, $\left|w^p\right|_{1,\Omega}$ and $\left|\varphi^p\right|_{1,\Omega}$. We therefore need to estimate these factors. We first start with this last one. Using the identities (25) and (29) we may write

$$\int_\Omega|\boldsymbol{curl}\ \varphi^p|^2 = \sum_{E\in\mathcal{E}_{ph}}\int_E J^p_{E,t}\cdot(\varphi^p - I_C\varphi^p).$$

Using the approximation error estimate (10) and the definition of the *a posteriori* error estimator we get

$$\|\boldsymbol{curl}\ \varphi^p\|^2 \lesssim \eta^p|\varphi^p|_{1,\Omega}.$$

With the help of (27) if $d = 3$, we conclude that

$$|\varphi^p|_{1,\Omega} \lesssim \eta^p. \tag{47}$$

For the estimation of the norm of $\nabla_h(e^p - w^p)$, we start with

$$\|\nabla_h(e^p - w^p)\|^2 = \int_\Omega\nabla_h(e^p - w^p)\cdot\nabla_h(e^p - w^p).$$

Using the Helmholtz decomposition (20) we then write

$$\|\nabla_h(e^p - w^p)\|^2 = \int_\Omega\nabla_h(e^p - w^p)\cdot\boldsymbol{curl}\ \varphi^p.$$

By Lemma 3.7 and Green's formula (recalling that $w^p = 0$ on Γ), we arrive at

$$\|\nabla_h(e^p - w^p)\|^2 = \sum_{E\in\mathcal{E}_{ph}} \int_E J^p_{E,t} \cdot (\varphi^p - I_C\varphi^p).$$

Using the estimates (44) and (47) we obtain

$$\|\nabla_h(e^p - w^p)\| \lesssim \eta^p. \tag{48}$$

By the triangular inequality we have

$$\|\nabla w^p\| \le \|\nabla_h(w^p - e^p)\| + \|\nabla_h e^p\|,$$

and by the well-known estimate $(a+b)^2 \le 2a^2 + 2b^2$, valid for any real numbers a, b, we obtain

$$\|\nabla w^p\|^2 \le 2\|\nabla_h(w^p - e^p)\|^2 + 2\|\nabla_h e^p\|^2.$$

By the estimate (48) we arrive at

$$\|\nabla w^p\|^2 \le C(\eta^p)^2 + 2\|\nabla_h e^p\|^2, \tag{49}$$

for some constant $C > 0$ depending only on the minimal angle of T_{ph}.

We are now able to conclude: Using the estimates (47), (48) and Young's inequality in (46), we may write

$$\int_\Omega |e^p|^2 + \tau_p \int_\Omega |\nabla_h e^p|^2 \le (e^{p-1}, e^p) + Ch_p\|e^p - e^{p-1}\|\eta^p + C\tau_p\|\nabla_h e^p\|\eta^p + C\tau_p((\eta^p)^2 + \xi^p)^2) + \frac{1}{8}\tau_p\,|w^p|^2_{1,\Omega},$$

for some constant $C > 0$ depending only on the minimal angle of T_{ph}.

Using the estimate (49) for the estimate of the term $|w^p|^2_{1,\Omega}$ and again Young's inequality, we finally arrive at

$$\begin{aligned}\int_\Omega |e^p|^2 + \tau_p \int_\Omega |\nabla_h e^p|^2 &\le (e^{p-1}, e^p) + \frac{1}{2}\|e^p - e^{p-1}\|^2 + Ch_p^2(\eta^p)^2 + C\tau_p((\eta^p)^2 + \xi^p)^2) + \frac{\tau_p}{2}\|\nabla_h e^p\|^2 \\ &\le \frac{1}{2}\|e^p\|^2 + \frac{1}{2}\|e^{p-1}\|^2 + C(\max\{h_p^2, \tau_p\}(\eta^p)^2 + \tau_p(\xi^p)^2) + \frac{\tau_p}{2}\|\nabla_h e^p\|^2,\end{aligned}$$

for some constant $C > 0$ depending only on the minimal angle of T_{ph}. This estimate is equivalent to

$$\|e^p\|^2 + \tau_p \int_\Omega |\nabla_h e^p|^2 \le \|e^{p-1}\|^2 + 2C(\max\{h_p^2, \tau_p\}(\eta^p)^2 + \tau_p(\xi^p)^2),$$

and we conclude by taking the sum on $p = 1, \ldots, n$. □

Corollary 5.3 (second upper error bound)**.** *The next estimate holds*

$$\|\partial_t(u_\tau - u_{h\tau})\|^2_{L^2(0,t_n;H^{-1}(\Omega)} \lesssim \sum_{p=1}^n \max\{h_p^2, \tau_p\}(\eta^p)^2 + \left\|e^0\right\|^2 + \|\nabla_h e^0\|^2 + \sum_{p=1}^n \tau_p(\xi^p)^2. \tag{50}$$

Proof. By definition we have

$$\|\partial_t(u_\tau - u_{h\tau})(t)\|_{H^{-1}(\Omega)} = \sup_{v\in H^1_0(\Omega)} \frac{(\partial_t(u_\tau - u_{h\tau})(t), v)}{\|v\|_{1,\Omega}}.$$

Using the property

$$\partial_t(u_\tau - u_{h\tau})(t) = \frac{e^p - e^{p-1}}{\tau_p}, \forall t \in (t_{p-1}, t_p),$$

and the semi-discrete equation (4), for any $t \in (t_{p-1}, t_p)$ we may write

$$(\partial_t(u_\tau - u_{h\tau})(t), v) = R^p(v) - (\nabla_h e^p, \nabla v),$$

where the residual R^p is defined by

$$R^p(v) = (f^p, v) - \left(\frac{u_h^p - u_h^{p-1}}{\tau_p}, v\right) - (\nabla_h u_h^p, \nabla v), \forall v \in H_0^1(\Omega).$$

As (5) implies that

$$R^p(v_h) = 0, \forall v_h \in V_{nh}^0,$$

the above identity becomes

$$(\partial_t(u_\tau - u_{h\tau})(t), v) = R^p(v - v_h) - (\nabla_h e^p, \nabla v), \forall v_h \in V_{ph}^0, t \in (t_{p-1}, t_p).$$

Taking $v_h = I_C v$, applying Green's formula componentwise, and using the estimate (12) we get

$$|(\partial_t(u_\tau - u_{h\tau})(t), v)| \lesssim (\eta^p + \|\nabla_h e^p\|)\|\nabla v\|, \forall t \in (t_{p-1}, t_p).$$

This estimate and Poincaré-Friedrichs' inequality lead to

$$\|\partial_t(u_\tau - u_{h\tau})(t)\|_{H^{-1}(\Omega)} \lesssim \eta^p + \|\nabla_h e^p\|, \forall t \in (t_{p-1}, t_p).$$

The conclusion then follows from the estimate (41). □

5.2. **Lower error bound**

We establish the lower error bound of the estimator η_K^p in a more or less standard way (see [14,20]). Since we consider a nonstationary problem, we further need the following assumption (see [9,22]), that is easily checked in an adaptive context:

Assumption 5.4. *For all $1 \le p \le N$, there exists a conforming triangulation $\tilde{T}_{ph}$ such that each element K of $T_{p-1,h}$ or of T_{ph} is the union of elements $\tilde{K}$ of $\tilde{T}_{ph}$ such that $h_K \sim h_{\tilde{K}}$.*

For our convenience we reformulate Corollary 3.5 in the following way:

Lemma 5.5. *For all $v \in H_0^1(\Omega)$, $\varphi \in H^1(\Omega)$ if $d = 2$ and $\varphi \in H^1(\Omega)^3$ if $d = 3$ we have the following identity:*

$$\int_\Omega (e^p - e^{p-1})v + \tau_p \sum_{K \in T_{ph}} \int_K \nabla_h e^p \cdot (\nabla v + \boldsymbol{curl}\, \varphi) = \tau_p \int_\Omega (f^p - f_h^p)v + \tau_p \sum_{K \in T_{ph}} \int_K \left(f_h^p - \frac{u_h^p - u_h^{p-1}}{\tau_p}\right) v + \tau_p \sum_{E \in \mathcal{E}_{ph}} \int_E (J_{E,n}^p v + J_{E,t}^p \cdot \varphi).$$

Theorem 5.6 (local lower error bound)**.** *If Assumption 5.4 holds, then for all $1 \le p \le N$, it holds*

$$\eta_K^p \lesssim h_K \left\| \frac{e^p - e^{p-1}}{\tau_p} \right\|_{\omega_K} + \|\nabla_h e^p\|_{\omega_K} + \xi_K^p. \tag{51}$$

Proof. **Element residual** Fix an arbitrary element $K \in \tilde{T}_{ph}$ and define

$$r_K^p := \left(f_h^p - \frac{u_h^p - u_h^{p-1}}{\tau_p} \right)_{|K}, \quad w_K^p := b_K r_K^p,$$

where $b_K = \lambda_1^K \lambda_2^K \lambda_3^K$ is the standard bubble function associated with K (see *e.g.* [20]). Standard inverse inequalities (*cf.* [20]) and Lemma 5.5 with $v = w_K^p$ and $\varphi = 0$ give

$$\begin{aligned} \|r_K^p\|_K^2 \sim \int_K r_K^p w_K^p &= \int_K \left(f_h^p - \frac{u_h^p - u_h^{p-1}}{\tau_p} \right) w_K^p \\ &= \int_K \left(\frac{e^p - e^{p-1}}{\tau_p} w_K^p + \nabla_h e^p \cdot \nabla w_K^p - (f^p - f_h^p) w_K^p \right) \\ &\lesssim \left(\left\| \frac{e^p - e^{p-1}}{\tau_p} \right\|_K + h_K^{-1} |e^p|_{1,K} + \|f^p - f_h^p\|_K \right) \|r_K^p\|_K. \end{aligned}$$

This proves the estimate

$$h_K \|r_K^p\|_K \lesssim h_K \left\| \frac{e^p - e^{p-1}}{\tau_p} \right\|_K + |e^p|_{1,K} + h_K \|f^p - f_h^p\|_K, \forall K \in \tilde{T}_{ph}. \tag{52}$$

Now for $K \in T_{ph}$, the Assumption 5.4 yields

$$h_K^2 \|r_K^p\|_K^2 \lesssim \sum_{\tilde{K} \in \tilde{T}_{ph} : \tilde{K} \subset K} h_{\tilde{K}}^2 \|r_{\tilde{K}}^p\|_{\tilde{K}}^2.$$

Using the estimate (52) and the fact that $h_{\tilde{K}} \leq h_K$ for $\tilde{K} \subset K$ we have proved that

$$h_K \|r_K^p\|_K \lesssim h_K \left\| \frac{e^p - e^{p-1}}{\tau_p} \right\|_K + |e^p|_{1,K} + \xi_K, \forall K \in T_{ph}. \tag{53}$$

Tangential jump. Next we consider an arbitrary edge/face E of T_{ph} and define

$$w_E^p := b_E J_{E,t}^p,$$

where b_E is the standard bubble function associated with E (see *e.g.* [20]).

Lemma 5.5 with $v = 0$ and $\varphi = w_E^p$ and inverse inequalities give

$$\begin{aligned} \left\| J_{E,t}^p \right\|_E^2 &\sim \sum_{K \subset \omega_E} \int_K \nabla_h e^p \cdot \boldsymbol{curl}\, w_E^p \\ &\lesssim \|\nabla_h e^p\|_{\omega_E} \|\nabla w_E^p\|_{\omega_E} \\ &\lesssim h_E^{-1/2} \left\| J_{E,t}^p \right\|_E \|\nabla_h e^p\|_{\omega_E}. \end{aligned}$$

This proves that

$$h_E^{1/2} \left\| J_{E,t}^p \right\|_E \lesssim \|\nabla_h e^p\|_{\omega_E}. \tag{54}$$

Normal jump. Similarly for an interior arbitrary edge/face E of T_{ph}, we define

$$w_E^p := b_E J_{E,n}^p.$$

Using inverse estimates and Lemma 5.5 with $v = w_E^p$ and $\varphi = 0$ we obtain

$$\left\| J_{E,n}^p \right\|_E \lesssim h_E^{1/2} \left\| \frac{e^p - e^{p-1}}{\tau_p} \right\|_{\omega_E} + h_E^{-1/2} \|\nabla_h e^p\|_{\omega_E} + h_E^{1/2} \|f^p - f_h^p\|_{\omega_E} + h_E^{1/2} \left\| f_h^p - \frac{u_h^p - u_h^{p-1}}{\tau_p} \right\|_{\omega_E}.$$

With the help of (53) this yields

$$h_E^{1/2} \left\| J_{E,n}^p \right\|_E \lesssim h_E \left\| \frac{e^p - e^{p-1}}{\tau_p} \right\|_{\omega_E} + \|\nabla_h e^p\|_{\omega_E} + h_E \|f^p - f_h^p\|_{\omega_E}. \tag{55}$$

The conclusion follows from the estimates (53), (54) and (55). □

Corollary 5.7 (second local lower error bound)**.** *If Assumption 5.4 holds, then for all* $1 \leq p \leq N$*, it holds*

$$(\eta^p)^2 \lesssim \|\partial_t(u_\tau - u_{h\tau})\|_{H^{-1}(\Omega)}^2 + \|\nabla_h e^p\|^2 + (\xi^p)^2. \tag{56}$$

Proof. As

$$\partial_t(u_\tau - u_{h\tau})(t) = \frac{e^p - e^{p-1}}{\tau_p}, \forall t \in (t_{p-1}, t_p),$$

in the above proof we need to replace the local L^2-norm of $\frac{e^p - e^{p-1}}{\tau_p}$ by its global $H^{-1}(\Omega)$-norm. For that purpose in Lemma 5.5 we take $\varphi = 0$ and

$$v = \sum_{\tilde{K} \in \tilde{T}_{ph}} h_{\tilde{K}}^2 r_{\tilde{K}}^p b_{\tilde{K}},$$

which yields, with the help of the assumption 5.4,

$$\sum_{K \in T_{ph}} h_K^2 \|r_K^p\|_K^2 \lesssim (\|\partial_t(u_\tau - u_{h\tau})\|_{H^{-1}(\Omega)} + \|\nabla_h e^p\|) \|\nabla v\| + \sum_{K \in T_{ph}} \|f^p - f_h^p\|_K \|v\|_K.$$

Standard inverse inequalities lead to

$$\sum_{K \in T_{ph}} h_K^2 \|r_K^p\|_K^2 \lesssim \|\partial_t(u_\tau - u_{h\tau})\|_{H^{-1}(\Omega)}^2 + \|\nabla_h e^p\|^2 + (\xi^p)^2.$$

Similarly for the estimate of the normal jump, we use Lemma 5.5 with $\varphi = 0$ and

$$v = \sum_{E \in \mathcal{E}_{ph}^{int}} h_E J_{E,n}^p b_E,$$

to get

$$\sum_{E \in \mathcal{E}_{ph}^{int}} h_E \left\| J_{E,n}^p \right\|_E^2 \lesssim \|\partial_t(u_\tau - u_{h\tau})\|_{H^{-1}(\Omega)}^2 + \|\nabla_h e^p\|^2 + (\xi^p)^2.$$

These estimates and (54) allow to conclude. □

6. *A posteriori* analysis of the full discretization

For all $n = 1, \cdots, N$, denote the full error $E(t_n)$ at time t_n by

$$E(t_n)^2 = \|u(t_n) - u_h^n\|^2 + \|u^n - u_h^n\|^2 + \|\partial_t(u - u_\tau)\|^2_{L^2(0,t_n;H^{-1}(\Omega))} + \|\partial_t(u_\tau - u_{h\tau})\|^2_{L^2(0,t_n;H^{-1}(\Omega))} + \int_0^{t_n} \|\nabla_h(u - u_\tau)(\cdot, s)\|^2 \,\mathrm{d}s + \int_0^{t_n} \|\nabla_h(u_\tau - u_{h\tau})(\cdot, s)\|^2 \,\mathrm{d}s.$$

Combining the results from the previous sections, we get the following global upper and lower bounds:

Theorem 6.1 (full error bounds)**.** *For any $n = 1, \cdots, N$, the next upper error bound holds:*

$$E(t_n)^2 \lesssim \sum_{p=1}^{n} \big((\eta_t^p)^2 + \max\{h_p^2, \tau_p\}(\eta^p)^2\big) + \|f - \pi_\tau f\|^2_{L^2(0,t_n;H^{-1}(\Omega))} + \sum_{p=1}^{n} \tau_p(\xi^p)^2 + \|e^0\|^2 + \tau_0\|\nabla_h e^0\|^2. \quad (57)$$

If moreover Assumption 5.4 holds, then for any $n = 1, \cdots, N$, the next lower error bound holds:

$$\sum_{p=1}^{n} \big((\eta_t^p)^2 + \tau_p(\eta^p)^2\big) \lesssim E(t_n)^2 + \|f - \pi_\tau f\|^2_{L^2(0,t_n;H^{-1}(\Omega))} + \sum_{p=1}^{n} \tau_p(\xi^p)^2. \quad (58)$$

Proof. Let us start with the upper error bound. First by Theorem 4.1 and Corollary 4.2, we have

$$E(t_n)^2 \lesssim \sum_{p=1}^{n} (\eta_t^p)^2 + \|(u_\tau - u_{h\tau})(t_n)\|^2 + \int_0^{t_n} \|\nabla_h(u_\tau - u_{h\tau}(s)\|^2 \,\mathrm{d}s + \|\partial_t(u_\tau - u_{h\tau})\|^2_{L^2(0,t_n;H^{-1}(\Omega))} + \|f - \pi_\tau f\|^2_{L^2(0,t_n;H^{-1}(\Omega))}.$$

As $(u_\tau - u_{h\tau})(t_n) = u^n - u_h^n = e^n$ and

$$|\nabla_h(u_\tau - u_{h\tau})(s)| \le |\nabla_h e^{p-1}| + |\nabla_h e^p|, \forall s \in [t_{p-1}, t_p],$$

the above estimate may be transformed into

$$E(t_n)^2 \lesssim \sum_{p=1}^{n} (\eta_t^p)^2 + \|e^n\|^2 + \sum_{p=0}^{n} \tau_p\|\nabla_h e^p\|^2 + \|\partial_t(u_\tau - u_{h\tau})\|^2_{L^2(0,t_n;H^{-1}(\Omega))} + \|f - \pi_\tau f\|^2_{L^2(0,t_n;H^{-1}(\Omega))}.$$

We conclude using Theorem 5.2 and Corollary 5.3.

We now pass to the lower error bound. Summing the square of (40) on $p = 1, \cdots, n$, we get

$$\sum_{p=1}^{n} (\eta_t^p)^2 \lesssim \int_0^{t_n} \|\nabla_h e_\tau(s)\|^2 \,\mathrm{d}s + \|\partial_t e_\tau\|^2_{L^2(0,t_n;H^{-1}(\Omega))} + \sum_{p=0}^{n} \tau_p(\|\nabla_h(u^p - u_h^p)\|^2 + \|\nabla_h(u_h^{p-1} - u_h^{p-1})\|^2) + \|f - \pi_\tau f\|^2_{L^2(0,t_n;H^{-1}(\Omega))}.$$

By the estimate (37), we obtain

$$\sum_{p=1}^{n} (\eta_t^p)^2 \lesssim E(t_n)^2 + \|f - \pi_\tau f\|^2_{L^2(0,t_n;H^{-1}(\Omega))}. \quad (59)$$

On the other hand, by Corollary 5.7, we have

$$\sum_{p=1}^{n} \tau_p(\eta^p)^2 \lesssim \|\partial_t(u_\tau - u_{h\tau})\|^2_{L^2(0,t_n;H^{-1}(\Omega))} + \sum_{p=1}^{n} \tau_p(\|\nabla_h(u^p - u_h^p)\|^2 + (\xi^p)^2).$$

Again thanks to (37), we obtain

$$\sum_{p=1}^{n} \tau_p(\eta^p)^2 \lesssim E(t_n)^2 + \sum_{p=1}^{n} \tau_p(\xi^p)^2. \tag{60}$$

The estimate (58) directly follows from (59) and (60). □

Remark 6.2. If we assume that

$$h_p^2 \lesssim \tau_p, \forall 1 \leq p \leq N, \tag{61}$$

then Theorem 6.1 states that the error $E(t_n)$ is equivalent to the global error estimator

$$\left(\sum_{p=1}^{n} \left((\eta_t^p)^2 + \tau_p(\eta^p)^2\right)\right)^{1/2},$$

up to approximation terms. Therefore this global error estimator may be used for an adaptive algorithm that has to respect (61).

7. Numerical experiments

The following experiments will confirm our theoretical analysis. Since our main contribution concerns the spatial error estimator, we only concentrate our efforts to its validity. The first example is used to confirm the efficiency and reliability of our spatial error estimator. The second example illustrate the use of our spatial estimator by presenting a spatial adaptive algorithm for a solution having a singular behaviour in space.

7.1. **Test 1**

This example consists in solving the two dimensional heat equation on the unit square $\Omega =]0,1[\times]0,1[$. Here, we first use the Crouzeix-Raviart element on uniform meshes $T_{ph} = T_h$ obtained by dividing each segment by n subintervals and dividing each obtained rectangle into two triangles (see Fig. 2).

The tests are performed with $T = 1s$ and the following exact solution u:

$$u(x,y,t) = e^{-t}xy(x-1)(y-1) \text{ in } \Omega\times]0,1[,$$

so that $u_0(x,y) = xy(x-1)(y-1)$ in Ω and $u(.,t)_{|\Gamma} = 0$, for all $t \in]0,1[$. We fix $\tau_p = 0.1s$, then $N = T/\tau_p = 10$. All numerical results will be presented at the final time $T = 1s$ ($N = 10$).

First, we check that the numerical solution u_h^N converges towards the exact one. For that purpose, in Figure 3, we have plotted $\left\|\nabla_h e^N\right\|$ as a function of the degrees of freedom ($DoF = 3n^2 - 4n + 2$ with $h = 1/n$). A double logarithmic scale was used such that the slope of the curves yields the order of convergence. As we can see, this figure underlines the theoretical predicted optimal order of convergence h (see [10]).

Now we investigate the main theoretical results which are the upper and lower error bounds (41) and (51).

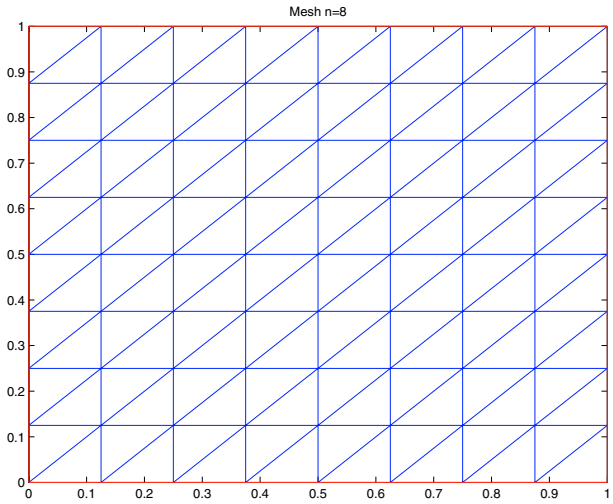

FIGURE 2. The uniform mesh on the unit square with $n = 8$.

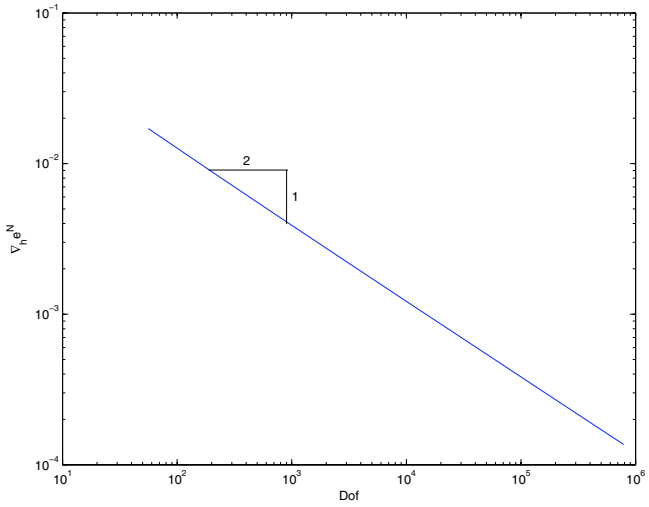

FIGURE 3. $\left\|\nabla_h e^N\right\|$ as a function of DoF for uniform meshes.

7.1.1. *Reliability of the spatial estimator*

First, we define the ratio of the left-hand side and the right-hand side of the inequality (41) at the last time $T = 1s$:

$$q_{up}^N = \frac{\left\|e^N\right\|^2 + \sum_{p=1}^{N} \tau_p \left\|\nabla_h e^p\right\|^2}{\left\|e^0\right\|^2 + \sum_{p=1}^{N} \tau_p \sum_{K \in T_{ph}} ((\eta_K^p)^2 + h_K^2 \left\|f^p - f_h^p\right\|_K^2)}.$$

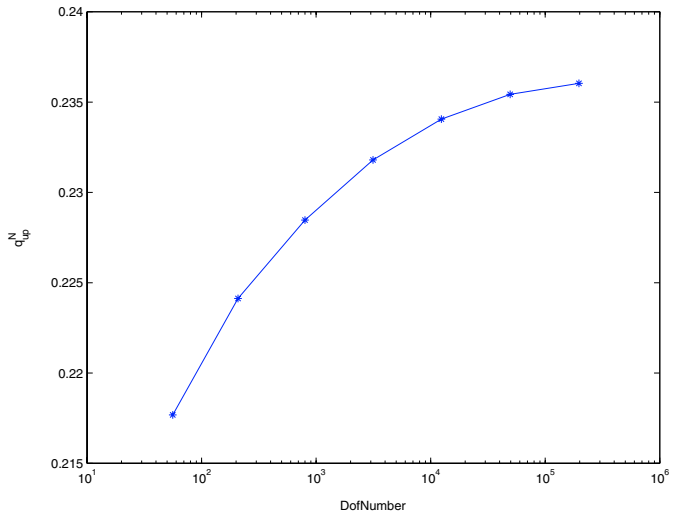

FIGURE 4. q^N_{up} wrt DoF for uniform meshes.

TABLE 1. q^N_{up} and q^N_{low} wrt DoF for uniform meshes.

n	DoF	q^N_{up}	q^N_{low}
4	56	0.21768	2.0782
8	208	0.22413	2.5714
16	800	0.22847	2.9010
32	3136	0.23180	3.1265
64	12416	0.23406	3.2208
128	49408	0.23543	3.2843
256	197120	0.23604	3.2930
512	787456	0.23617	3.2975

q^N_{up} is referred as the *effectivity index*. It measures the *reliability* of the estimator and is related to the global upper error bound. From Theorem 5.2, the ratio q^N_{up} is bounded from above. This can be confirmed by our numerical results presented in Figure 4 and Table 1. Hence, the spatial estimator is reliable.

7.1.2. *Efficiency of the spatial estimator*

Now, we define the (larger) ratio of the left-hand side and the right-hand side of the inequality (51) at the final time $T = 1s$:

$$q^N_{low} = \max_{K \in T_{ph}} \frac{\eta^N_K}{h_K \left\| \dfrac{e^N - e^{N-1}}{\tau_p} \right\|_{\omega_K} + \|\nabla_h e^N\|_{\omega_K} + h_K \left\| f^N - f^N_h \right\|_{\omega_K}}.$$

q^N_{low} is related to the local lower error bound and measures the *efficiency* of the estimator. According to Figure 5 (see also Tab. 1), q^N_{low} is bounded from above as theoretically predicted in Theorem 5.6. Therefore our spatial estimator is also efficient.

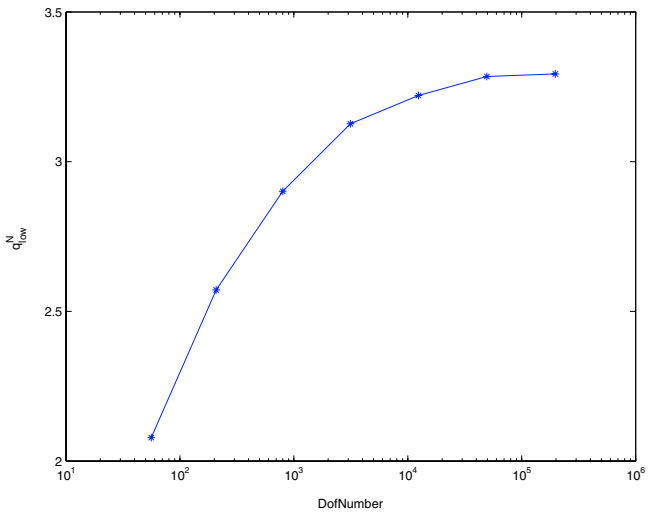

FIGURE 5. q^N_{low} wrt DoF for uniform meshes.

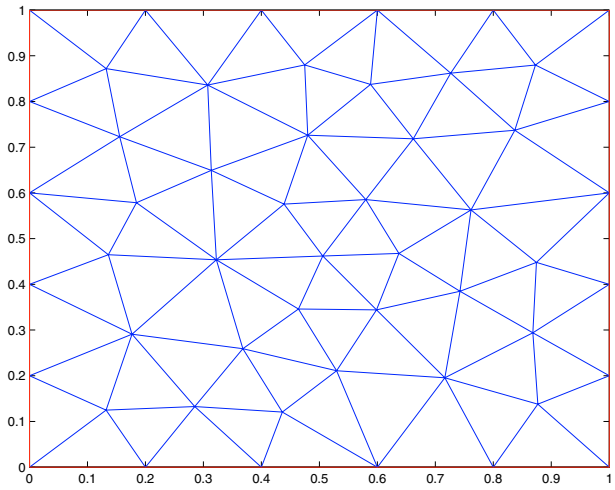

FIGURE 6. The non structured mesh on the unit square with $h = 0.2$.

7.1.3. *Non structured meshes*

In order to validate the reliability and efficiency of our spatial error estimator, we have approximated the same problem as before with the same elements but on different non structured meshes obtained by starting from a rough non structured mesh of size 0.2 (see Fig. 6) and by dividing each triangle into 4 triangles by the standard regular refinements [20]. Figures 7 and 8 (see also Tab. 2) show respectively the ratios q^N_{up} and q^N_{low} with respect to the degrees of freedom. Again we may conclude that both ratios are bounded from above and consequently our spatial error estimator is reliable and efficient.

7.2. **Dependence of the error**

From our previous considerations, the error between the exact solution and its approximated one is expected to depend on the space and/or time discretization. In order to illustrate this phenomenon, as in [17], we exhibit

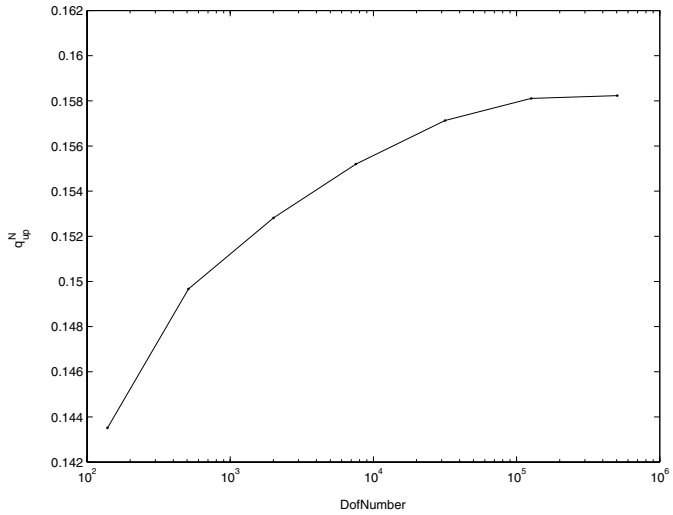

FIGURE 7. q^N_{up} wrt DoF for the non structured meshes.

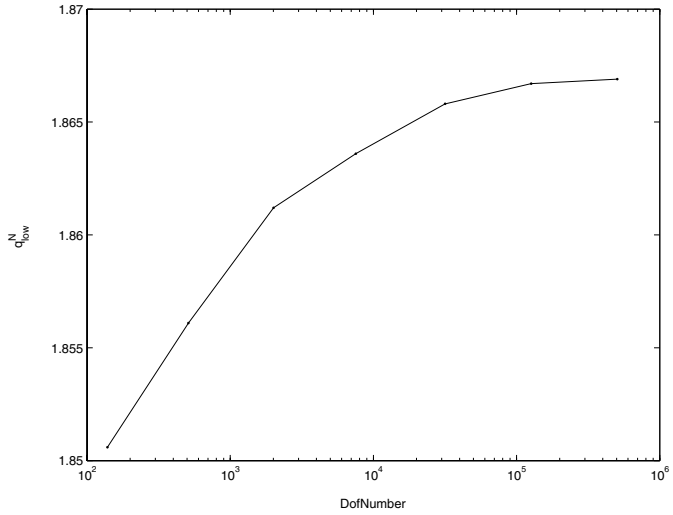

FIGURE 8. q^N_{low} wrt DoF for the non structured meshes.

an example where the error due to the time discretization is more important than the error due to the space discretization, and another example where the converse phenomenon appears. For that purpose we consider the problem (1) for $\Omega =]0,1[\times]0,1[$ and $T = 1s$, with the exact solutions u_1 and u_2 defined by:

$$u_1(x,y,t) = \sin(10\pi t/2)\sin(\pi x/2)\sin(\pi y/2),$$

and

$$u_2(x,y,t) = \sin(10\pi t/2)\sin(10\pi x/2)\sin(10\pi y/2).$$

The numerical results are shown in Tables 3 and 4, where we present the values of the space indicator η, the time indicator η_t, the error $\|e\| := (\sum_{p=1}^N \tau_p \|\nabla_h e^p\|^2)^{1/2}$ and the spatial effectivity index q^N_{up} for different uniform triangulations and constant time steps. In the first case, we can conclude that the error is mainly due to the

TABLE 2. q_{up}^N and q_{low}^N wrt DoF for the non structured meshes.

h	DoF	q_{up}^N	q_{low}^N
0.2	139	0.14351	1.8506
0.1	512	0.14967	1.8561
0.05	2008	0.15282	1.8612
0.025	7952	0.15520	1.8636
0.0125	31648	0.15713	1.8658
0.00625	126272	0.15811	1.8667
0.003125	504448	0.15823	1.8669

TABLE 3. Convergence results when using uniform triangulations and constant time steps for the first example.

$h=1/n$	$\mathrm{d}t$	η	η_t	$\|e\|$	q_{up}^N	$h=1/n$	$\mathrm{d}t$	η	η_t	$\|e\|$	q_{up}^N
0.1	0.1	0.096	0.65	0.31	3.6	0.1	0.05	0.062	0.34	0.19	3.3
0.05	0.1	0.051	0.65	0.31	3.6	0.05	0.05	0.031	0.34	0.19	3.3
0.025	0.1	0.025	0.65	0.31	3.6	0.025	0.05	0.016	0.34	0.19	3.3
0.0125	0.1	0.012	0.65	0.30	3.7	0.0125	0.05	0.008	0.34	0.19	3.3
0.1	0.025	0.043	0.18	0.11	3.0	0.1	0.0125	0.041	0.09	0.06	2.7
0.05	0.025	0.022	0.18	0.10	3.1	0.05	0.0125	0.021	0.09	0.06	2.7
0.025	0.025	0.011	0.18	0.10	3.1	0.025	0.0125	0.010	0.09	0.05	2.8
0.0125	0.025	0.005	0.18	0.10	3.1	0.0125	0.0125	0.005	0.09	0.05	2.8

TABLE 4. Convergence results when using uniform triangulations and constant time steps for the second example.

$h=1/n$	$\mathrm{d}t$	η	η_t	$\|e\|$	q_{up}^N	$h=1/n$	$\mathrm{d}t$	η	η_t	$\|e\|$	q_{up}^N
0.1	0.1	4.8	7.5	5.2	2.9	0.1	0.05	4.8	3.9	4.9	1.4
0.05	0.1	2.6	7.2	2.9	5.8	0.05	0.05	2.6	3.8	2.5	2.9
0.025	0.1	1.3	7.2	2.1	7.9	0.025	0.05	1.3	3.8	1.4	7.9
0.0125	0.1	0.65	7.1	1.6	8.4	0.0125	0.05	0.65	3.8	0.83	8.1
0.1	0.025	4.8	1.9	5.4	0.7	0.1	0.0125	4.8	1.0	5.4	0.5
0.05	0.025	2.6	1.9	2.7	1.5	0.05	0.0125	2.6	1.0	2.7	0.8
0.025	0.025	1.3	1.9	1.3	2.8	0.025	0.0125	1.3	1.0	1.3	1.3
0.0125	0.025	0.65	1.9	0.69	5.5	0.0125	0.0125	0.65	1.0	0.68	2.8

time discretization. Indeed from Table 3, we see that for a fixed time step and decreasing mesh sizes, the error is almost constant; while for a fixed mesh size and decreasing time steps, the error decreases. We moreover remark a close relationship between the error and the time indicator. For the second example, the error is mainly due to the time discretization, since we see converse relations between the error and the time steps

and mesh sizes; while we clearly detect a relationship between the error and the space indicator. For the first example q_{up}^N is correlated to the error, while for the second one, the distorsion comes for the approximation terms. Let us further remark that the numerical experiments bring to light that the indicator η_t is independent of h, while the indicator η is mainly independent of τ_p. This very important property of uncoupling the two error parts is effectively used in our adaptive algorithm described below, since the time (resp. space) refinements or unrefinements are (mainly) based on η_t (resp. η).

7.3. **An adaptive algorithm**

From our theoretical considerations and the examples of the previous subsection, an adaptive algorithm has to use appropriately the space indicator η, the time indicator η_t and the approximation error ξ. To design this algorithm, we first define the global indicator $\overline{\eta}$ as follows:

$$\overline{\eta} := \left(\sum_{n=1}^{N} \left((\eta_t^n)^2 + \tau_n (\eta^n)^2 + \tau_n (\xi^n)^2 \right) \right)^{1/2}.$$

For our approximated solution $u_{h\tau}$, we define a relative error estimator **Ind** by:

$$\mathbf{Ind}^2 = \frac{\overline{\eta}}{\int_0^T \|\nabla u_{h\tau}(\cdot, t)\|^2 \, \mathrm{d}t}. \tag{62}$$

Let a preset tolerance δ and a parameter $0 < \alpha < 1$ be given. The goal of our adaptive scheme is to generate a sequence of sub-intervals $[t_{n-1}, t_n]$ and mesh triangulations T_{nh}, $n = 1, \ldots, N$ such that **Ind**, defined by (62), is close to the preset of tolerance δ, in the sense that

$$(1 - \alpha)\delta \leq \mathbf{Ind} \leq (1 + \alpha)\delta. \tag{63}$$

To achieve these bounds, for all $n = 1, \cdots, N$, we define two local bounds: a left one $\mathbf{Lb}^n$ defined by

$$\mathbf{Lb}^n := (1 - \alpha)^2 \delta^2 \int_{t_{n-1}}^{t_n} \|\nabla u_{h\tau}(\cdot, t)\|^2 \, \mathrm{d}t \tag{64}$$

and a right one $\mathbf{Rb}^n$ defined by

$$\mathbf{Rb}^n := (1 + \alpha)^2 \delta^2 \int_{t_{n-1}}^{t_n} \|\nabla u_{h\tau}(\cdot, t)\|^2 \, \mathrm{d}t. \tag{65}$$

If, for all $n = 1, \cdots, N$, the conditions

$$\mathbf{Lb}^n \leq (\eta_t^n)^2 + \tau_n (\eta^n)^2 + \tau_n (\xi^n)^2 \leq \mathbf{Rb}^n \tag{66}$$

are satisfied, then summing from $n = 1$ to $n = N$, we obtain (63). Thus our algorithm consists in finding time steps and triangulations such that (66) holds for all n. This will be achieved by using the elements η^n and ξ^n to control the mesh sizes, and using ξ^n and η_t^n to control the time steps. This adaptive algorithm is presented in Table 5. Note that it is similar to the one proposed in [17].

In order to test our adaptive scheme, we consider two relevant examples. The first one when the heat equation (1) is considered in the unit square $]0, 1[\times]0, 1[$ with the exact solution defined by (see [17])

$$u(x, y, t) = \beta(t) * \exp(-50 * r^2(x, y, t)), \tag{67}$$

TABLE 5. The adaptive algorithm.

Set $T_{0h}, u_h^0, n = 1, t, \tau$	Initializations
Do while $t \leq T$	
Compute $(\eta^n)^2, (\eta_t^n)^2,$	
$(\xi^n)^2, \mathbf{Rb}^n, \mathbf{Lb}^n$	
If $\tau_n \frac{\xi^n}{2} + \eta_t^n < \mathbf{Lb}^n$	Current time step is to small
$\tau := 2\tau$	Same time iteration with bigger step
Else If $\tau_n \frac{\xi^n}{2} + \eta_t^n \leq \mathbf{Rb}^n$	
If $\tau_n(\eta^n + \frac{\xi^n}{2}) < \mathbf{Lb}^n$	Triangulation is too fine
Continue with criteria	
$\eta_K^n \leq 1.5 \min \eta_K^n$	
Else If $\tau_n(\eta^n + \frac{\xi^n}{2}) \leq \mathbf{Rb}^n$	Mesh Triangulation is correct
$t := t + \tau$	Incrementation of the current time step
$n = n + 1$	
Else	Mesh Triangulation is too coarse
Continue with criteria	Same time with finer triangulation
$\eta_K^n \geq 0.5 \max \eta_K^n$	
Else	Time step is too large
$\tau := \tau/2$	Same time iteration with smaller time step
End If	
Make T_{nh}	Generate the new triangulation
End Do	

TABLE 6. Some results for the Gaussian function with $\alpha = 0.5$.

Tolerance δ	***Time Steps***	***Ind***	$q_{\mathbf{up}}^{\mathbf{N}}$
1.0	10	0.62	1.4
0.5	20	0.33	1.3
0.25	40	0.17	1.2
0.125	80	0.084	1.2
0.0625	160	0.042	1.2

with $r^2(x, y, t) = (x - 0.4 * t - 0.3)^2 + (y - 0.4 * t - 0.3)^2$, and

$$\begin{cases} \beta(t) \quad = 1 - \exp(-50 * (0.98 * t + 0.01)^2) & \text{if } t < 0.5, \\ \beta(t) = 1 - \exp(-50 * (1 - 0.98 * t + 0.01)^2) & \text{else.} \end{cases} \tag{68}$$

This means that u is a Gaussian function which center moves from point (0.3, 0.3) at time $t = 0s$ to point (0.7, 0.7) at time $t = 1s$.

The obtained meshes at times 0.1, 0.5 and 1 are shown in Figures 9 to 11 respectively with the tolerance $\delta = 0.25$ and the parameter $\alpha = 0.5$. From these figures we may conclude that the meshes are refined in the region of a large gradient of the solution and then follow correctly the moving centers. Moreover from Table 6, we see for different tolerance parameters, that the effectivity index is quite close to 1.

As second example, we consider the heat equation (1) in the L-shape domain $]-1, 1[^2 \backslash]0, 1[\times]0, -1[$ with exact solution defined by

$$u(r, \theta) = \mathrm{e}^{-t} * r^{2/3} \sin\left(\frac{2}{3}\theta\right),$$

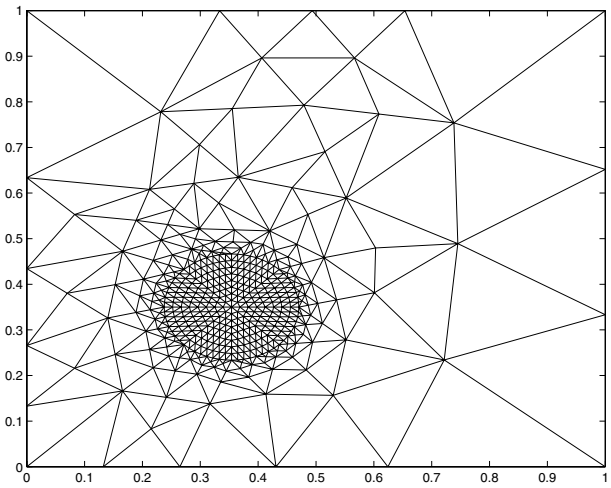

FIGURE 9. $n = 4$, $t_n = 0.1s$, $Nv = 442$.

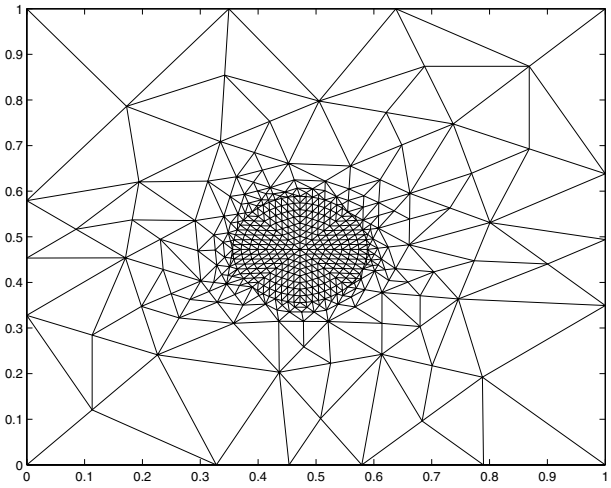

FIGURE 10. $n = 20$ $t_n = 0.5s$, $Nv = 462$.

where (r, θ) are polar coordinates centred at $(0, 0)$. In that case, u has a singular behaviour along the edge $(0, 0)\times]0, T[$.

Figures 12 to 14 present the obtained meshes at times 0.1, 0.5 and 1, respectively with the tolerance $\delta = 0.25$ and the parameter $\alpha = 0.5$. As expected the meshes are refined near the singular point, namely the origin. As previously Table 7 confirms a good effectivity index for different tolerance parameters.

8. CONCLUSION

We have proposed and analysed an *a posteriori* error estimator for the heat equation. Our investigations cover the nonconforming finite element discretization (Crouzeix-Raviart) on 2D and 3D domains. Much effort has been taken to prove the global upper and lower bound errors under quite realistic conditions. The main theoretical results, which are the upper and the lower spatial error bounds, are confirmed experimentally. More precisely the values q_{up}^N and q_{low}^N are bounded from above as other problem classes (*cf.* [14, 18]). Finally a

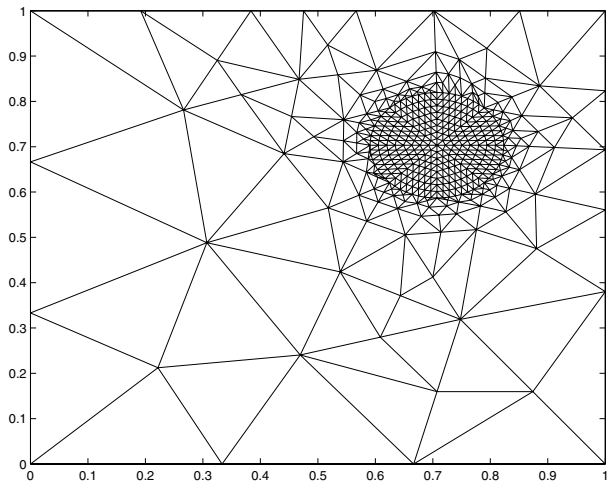

FIGURE 11. $n = 40$ $t_n = 1s$, $Nv = 470$.

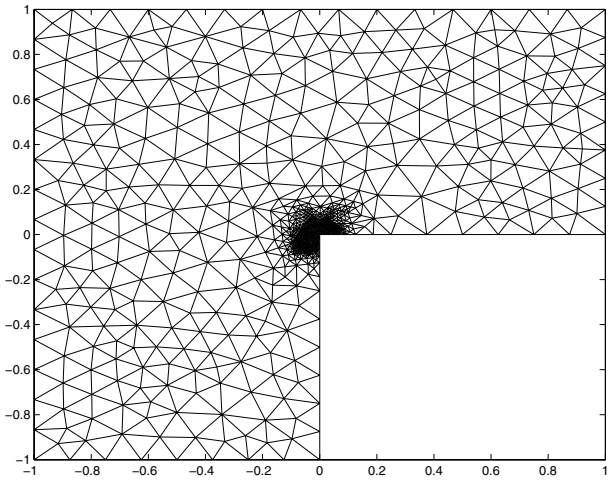

FIGURE 12. $n = 4$, $t_n = 0.1s$, $Nv = 836$.

TABLE 7. Some results for the singular function with $\alpha = 0.5$.

Tolerance δ	***Time Steps***	***Ind***	$q_{\mathbf{up}}^{\mathbf{N}}$
1.0	10	0.88	1.8
0.5	20	0.42	1.6
0.25	40	0.23	1.6
0.125	80	0.11	1.6
0.0625	160	0.055	1.5

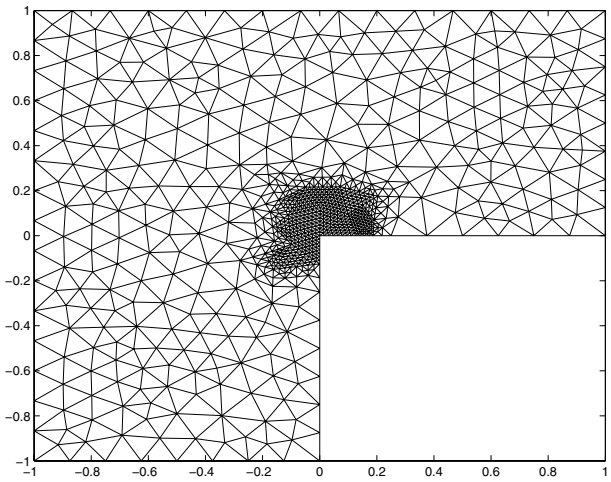

FIGURE 13. $n = 20$ $t_n = 0.5s$, $Nv = 872$.

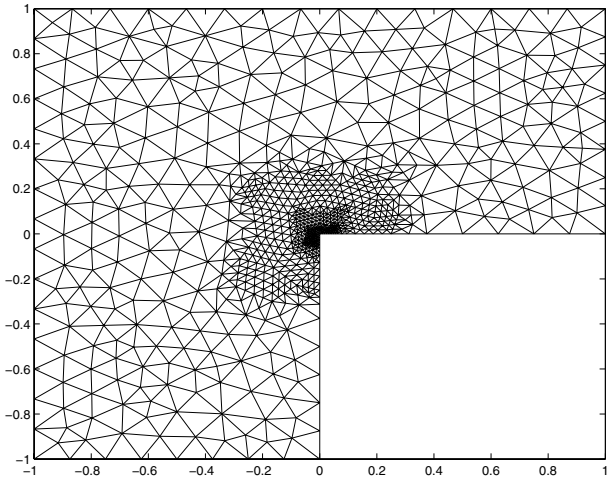

FIGURE 14. $n = 40$ $t_n = 1s$, $Nv = 874$.

space-time adaptive algorithm based on our error estimator is proposed and tested on two relevant examples. In both cases, the obtained meshes follows the singularity of the solution, which confirms the validity of our algorithm.

REFERENCES

[1] Y. Achdou, C. Bernardi and F. Coquel, *A priori* and *a posteriori* error analysis of finite volume discretizations of Darcy's equations. *Numer. Math.* **96** (2003) 17–42.
[2] G. Acosta and R.G. Durán, The maximum angle condition for mixed and non-conforming elements, Application to the Stokes equations. *SIAM J. Numer. Anal.* **37** (1999) 18–36.
[3] T. Apel, Anisotropic finite elements: Local estimates and applications. *Adv. Numer. Math.* Teubner, Stuttgart (1999).
[4] T. Apel and S. Nicaise, The inf-sup condition for some low order elements on anisotropic meshes. *Calcolo* **41** (2004) 89–113.
[5] T. Apel, S. Nicaise and J. Schröberl, A non-conforming finite element method with anisotropic mesh grading for the stokes problem in domains with edges. *IMA J. Numer. Anal.* **21** (2001) 843–856.

[6] A. Bergam, C. Bernardi and Z. Mghazli, *A posteriori* analysis of the finite element discretization of some parabolic problem. Preprint Laboratoire J.-L. Lions 01045, Université Paris 6 (2001).
[7] A. Bergam, C. Bernardi and Z. Mghazli, *A posteriori* analysis of the finite element discretization of a nonlinear parabolic equation. (2004) (to appear).
[8] C. Bernardi and B. Métivet, Indicateurs d'erreur pour l'équation de la chaleur. *Rev. Européenne Élém. Finis* **9** (2000) 425–438.
[9] C. Bernardi and R. Verfürth, *A posteriori* error analysis of the fully discretized time-dependent Stokes equations. *ESAIM: M2AN* **38** (2004) 437–455.
[10] P. Brenner, M. Crouzeix and V. Thomée, Single step methods for inhomogeneous linear differential equations in banach space. *RAIRO Anal. Numér.* **16** (1982) 5–26.
[11] P. Ciarlet, *The finite element method for elliptic problems.* North Holland (1996).
[12] P. Clément, Approximation by finite element functions using local regularization. *RAIRO Anal. Numér.* **2** (1975) 77–84.
[13] E. Creusé, G. Kunert and S. Nicaise, *A posteriori* error estimation for the Stokes problem: Anisotropic and isotropic discretizations. *Math. Models Methods Appl. Sci.* **14** (2004) 1297–1341.
[14] E. Dari, R. Durán, C. Padra and V. Vampa, *A posteriori* error estimators for nonconforming finite element methods. *RAIRO Modél. Math. Anal. Numér.* **30** (1996) 385–400.
[15] V. Girault and P.-A. Raviart, *Finite elements methods for Navier-Stokes equations, Theory and Algorithms.* Springer Series in Computational Mathematics, Berlin (1986).
[16] C. Johnson, Y.-Y. Nie and V. Thomée, An *a posteriori* error estimate and adaptive timestep control for a backward Euler discretization of a parabolic problem. *SIAM J. Numer. Anal.* **27** (1990) 277–291.
[17] M. Picasso, Adaptive finite elements for a linear parabolic problem. *Comput. Methods Appl. Mech. Engrg.* **167** (1998) 223–237.
[18] M. Picasso, An anisotropic error indicator based on Zienkiewicz-Zhu error estimator: Application to elliptic and parabolic problems. *SIAM J. Sci. Comput.* **24** (2003) 1328–1355.
[19] L.R. Scott and S. Zhang, Finite element interpolation of non-smooth functions satisfying boundary conditions. *Math. Comp.* **54** (1990) 483–493.
[20] R. Verfürth, *A review of a posteriori error estimation and adaptive mesh–refinement techniques.* Wiley-Teubner, Chichester, Stuttgart (1996).
[21] R. Verfürth, Error estimates for some quasi-interpolation operators. *ESAIM: M2AN* **33** (1999) 695–713.
[22] R. Verfürth, *A posteriori* error estimates for finite element discretization of the heat equation. *Calcolo* **40** (2003) 195–212.